ELSEVIER

Polymer 42 (2001) 7465–7475

polymer

www.elsevier.nl/locate/polymer

The fabrication of syndiotactic polystyrene/organophilic clay nanocomposites and their properties

Cheon Il Park[a], O Ok Park[a,*], Jae Gon Lim[b], Hyun Joon Kim[b]

[a]*Department of Chemical Engineering, Center for Advanced Functional Polymers, Korea Advanced Institute of Science and Technology, 373-1 Kusong-dong, Yusong-gu, Taejon 305-701, South Korea*

[b]*M-Project Team, R & D Center, Samsung General Chemicals Co. Ltd., 103-6 Moonji-dong, Yusong-gu, Taejon 305-714, South Korea*

Received 12 September 2000; received in revised form 22 November 2000; accepted 5 February 2001

Abstract

The fabrication of nanocomposite of syndiotactic polystyrene (sPS)/organophilic clay was conducted by melt intercalation. To avoid the decrease of interlayer spacing due to desorption of organic materials at high temperature, various amorphous styrenic polymers were introduced during the melt mixing process. The nanocomposites were fabricated via two different methods, one is the stepwise mixing method, which is the melt intercalation of amorphous styrenic polymers into organophilic clay followed by blending with sPS, and the other is the simultaneous mixing method, in which all components are melt mixed together. The microstructures of nanocomposites were investigated by X-ray diffraction (XRD) and transmission electron microscopy. The mechanical properties of the nanocomposites such as tensile strength, flexural modulus and izod impact strength were measured and discussed in relation to their microstructures. Both fabrication methods yielded the nanocomposites with different microstructures ranging from intercalated structure to exfoliated structure depending on the kind of amorphous styrenic polymers, which was revealed by the increase in interlayer spacing on X-ray spectrum. Amorphous polymers intercalated into the clay gallery previously is considered to play an important role in maintaining the intercalated or exfoliated structure without any contraction of interlayer spacing even at sPS melting temperature. The fabrication method also influenced the microstructure and mechanical properties, especially tensile strength. In the case of nanocomposites having intercalation structure, the stepwise mixing method yielded more obvious intercalation structure than the simultaneous mixing method so that the former method resulted in higher tensile strength. On the other hand, the nanocomposite having exfoliated structure showed similar mechanical properties between the two fabrication methods. © 2001 Published by Elsevier Science Ltd.

Keywords: Syndiotactic polystyrene; Clay; Nanocomposite

1. Introduction

Recently, polymer and clay hybrid, called nanocomposite, has been receiving special attention because of its various advantages in comparison to the traditional polymer composites. Common polymer composites usually involve a high amount of inorganic filler (more than 10% by weight) for imparting desired mechanical properties. However, this high content of inorganic filler brings about deteriorating properties, such as the increase in product density and the loss of tenacity due to the interfacial incompatibility between organic polymer and inorganic filler. Moreover, the processibility becomes worse, such as the high torque level of the mixing equipment and poor dispersion of inorganic filler, with the increase in filler content. On the other hand, nanocomposites show enhanced mechanical and thermal properties with even a small amount of clay because of the large contact area between polymer and clay through nanoscaled hybrid so that the nanocomposites are free from the above weak points of the traditional polymer composites. In addition, the layered structure of clay with high aspect ratio provides outstanding barrier properties. Low gas permeability, chemical resistance and flame retardance are attributed to the enhanced barrier properties of the nanocomposites [1,2]

Since the development of the Nylon6/montmorillonite nanocomposite by Toyota Motor Co. [3,4], a large number of studies on polymer/clay nanocomposites were performed [5–10]. However, nanocomposites using engineering thermoplastic as a polymer matrix were not sufficiently exploited. Almost all engineering plastics such as poly(ethylene terephthalate), poly(butylene terephthalate), poly(phenylene sulfide) and syndiotactic polystyrene (sPS) are reinforced by a high amount of glass fiber, which impart heat resistance and mechanical strength for the application in the field

* Corresponding author. Tel.: +82-42-869-3923; fax: +82-42-869-3910.
E-mail address: oopark@cais.kaist.ac.kr (O.O. Park).

0032-3861/01/$ - see front matter © 2001 Published by Elsevier Science Ltd.
PII: S0032-3861(01)00213-0

of construction material and electronic parts. Thus, the development of the nanocomposite of engineering thermoplastic/clay system is needed in view of the low product density and ease of processing.

In this article, we attempted to fabricate the nanocomposite of a sPS/clay system by melt intercalation. sPS has crystallinity and a high melting point (about 270°C) due to its stereo-regularity whereas atactic polystyrene (aPS) is an amorphous polymer [11]. Thus, sPS has heat resistance, chemical resistance and dimensional stability in addition to the properties of aPS, such as low specific gravity, electrical properties, hydrolytic stability, which makes sPS an important, new engineering thermoplastic. However, fabrication of nanocomposite by direct melt intercalation of sPS into organophilic clay has problems due to thermal instability of organic materials treated on inner layer surface of clay [12,13]. In general, clay should be swelled by alkyl ammonium material via cation exchange reaction between metal ion in clay gallery and alkyl ammonium ion in order for the polymer to penetrate into the clay gallery easily. However, the interaction between alkyl ammonium and silicate layer of clay is not thermally stable enough to resist high melt processing temperature of sPS, which makes the intercalation of sPS into the clay gallery difficult. To solve this problem, we approached an indirect way, i.e. melt intercalation of amorphous styrenic polymers into organophilic clay followed by blending with sPS. It is well known that amorphous styrenic polymers, such as aPS and clay nanocomposite could be obtained by melt intercalation [14]. Amorphous polystyrene is also known to be miscible or partially miscible with sPS [15,16]. Thus, it is expected that sPS nanocomposite can be obtained by blending sPS with previously melt intercalated amorphous styrenic polymers nanocomposites unless the intercalated structure disrupts at sPS melting temperature.

At first, the thermal stability of organophilic clay itself and amorphous styrenic polymers/clay nanocomposites is studied in order to probe the feasibility of the above fabrication method. The microstructures of the fabricated sPS nanocomposites are investigated by X-ray diffraction (XRD) and transmission electron microscope (TEM). The effect of mixing procedure on the properties of sPS nanocomposite is also investigated through two types of fabrication methods: one is the stepwise mixing explained above, and the other is the simultaneous mixing of all components. Finally, the mechanical properties of sPS nanocomposites are studied in relation with their microstructures.

2. Experimental

2.1. Materials

sPS, of which weight average molecular weight (M_w) was 313,200 was supplied by Samsung General Chem. aPS, styrene–maleic anhydride random copolymer (SMA) and maleic anhydride grafted styrene–ethylene–butylene–styrene block copolymer (SEBS-MA) were used as amorphous styrenic polymers. aPS ($M_w = 412{,}000$) was a commercial grade of Cheil Industry and SMA ($M_w = 224{,}000$), in which the composition of maleic anhydride (MA) was 7 wt% was purchased from Aldrich. SEBS-MA with grade name of Kraton FX1901 was the product of Shell Chem., in which 2 wt% of maleic anhydride was grafted to ethylene–butylene block. The organophilic clay of montmorillonite type (Cloisite® 15A) was supplied by Southern Clay Co. and used after drying in a vacuum oven at 80°C for two days. The surface of the organophilic clay is treated by dimethyl dihydrogenated tallow alkyl ammonium ion which consisted of 65 wt% of C_{18}, 30 wt% of C_{16} and 5 wt% of C_{14}. The cation exchange capacity (CEC) of the clay is 125 meq/100 g.

2.2. Fabrication of nanocomposite

In the case of stepwise mixing method, amorphous styrenic polymer and organophilic clay were mixed in a Brabender roller mixer at temperature of 200°C for 10 min with 50 rpm rotor speed. Polymer was inserted and melted completely in the mixing chamber, then organophilic clay was loaded into the molten polymer. After completion of mixing, the mixed composite was ejected from the mixing chamber, then cooled and crushed at room temperature. sPS nanocomposite was fabricated by blending sPS with the above product in a Brabender roller mixer at 280°C for 5 min with 50 rpm rotor speed. In the case of simultaneous mixing method, all components of sPS, amorphous styrenic polymer and organophilic clay were mixed together at room temperature, then melt mixed in a Brabender roller mixer at 280°C for 5 min with 50 rpm rotor speed.

For the thermal stability study, the organophilic clay or amorphous styrenic polymer/clay composite was heat treated around sPS melting temperature. The heat treatment of the organophilic clay was performed in the heating chamber of the rheometer for 10 min at temperature range from 200 to 280°C under air environment. And the amorphous styrenic polymer/clay composite fabricated in the Brabender roller mixer was mixed once more in a small vial of mini-molder (CSI co.) at 280°C with varying mixing time.

2.3. Measurements

XRD spectra were obtained using a Rigaku X-ray generator (CuKα radiation with $\lambda = 1.5406$ Å) with 2θ scan range of 0–10° at room temperature. The specimens of nanocomposite for XRD measurement were obtained in sheet form using a hydraulic press. The dispersion state and layered structure of clay were observed using a Jeol JEM-2000EX TEM. The specimens including SEBS-MA as a component were stained by the vapor of RuO_4 solution while other specimens were measured with no staining. Tensile properties, flexural modulus and izod impact

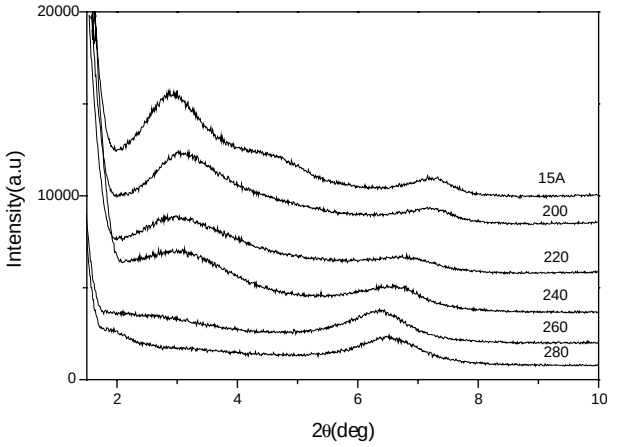

Fig. 1. XRD patterns of organophilic clay with increasing heat treatment temperatures (the number in the figure represents the heat treatment temperature, °C).

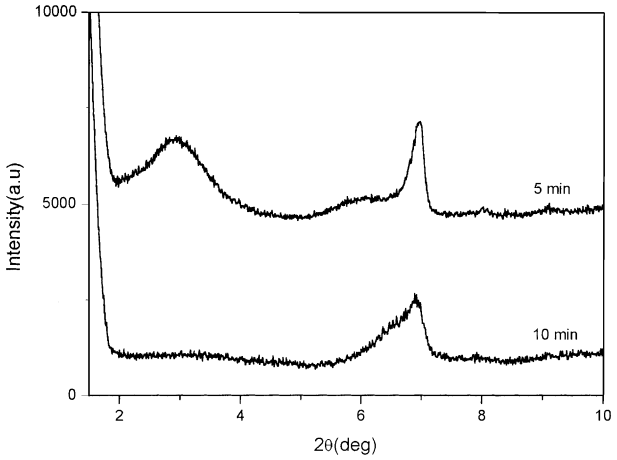

Fig. 2. XRD patterns of the sPS/15A (3 wt%) composite with different mixing time.

strength were measured as the mechanical properties of the nanocomposite. Tensile tests were performed using a universal tensile machine (Instron UTM) according to the test method of ASTM D 1708. The crosshead speed was 1 mm/min. Flexural modulus was also obtained using UTM according to the test method of ASTM D 790. The crosshead speed was 5 mm/min. Izod impact strength was obtained using an impact tester (Toyoseiki) with notched state according to the test method of ASTM D 256. All specimens for mechanical test were made by injection molding in a mini-molder (CSI).

3. Results and discussion

3.1. Thermal characterization of organophilic clay

For the fabrication of sPS nanocomposite via melt intercalation, organophilic clay should have thermal stability at high melt processing temperature of 280°C. For this purpose, it was investigated whether organophilic clay itself kept its layered structure with increasing heat treatment temperatures. Organophilic clay was heated in an oven of air environment for 10 min at a temperature range from 200 to 240°C, then *d*-space of clay layer was measured by XRD pattern. The XRD patterns of 15A in Fig. 1 show that the (001) peak at $2\theta = 2.97$ becomes broadened with the increase in temperature, then eventually shifts to $2\theta = 6.52$ at 260°C. This result indicates that the *d*-space decreases from 2.97 to 1.40 nm. The decrease in interlayer spacing is attributed to the degradation and desorption of organic materials in the gallery at high temperature, which was revealed in our laboratory [12]. By thermo-gravimetric analysis (TGA) experiment (not shown here), it was shown that about 70 wt% of the alkyl ammonium material was degraded at 280°C. This high amount of weight loss of organic material brings about the decrease in interlayer spacing, which hinders the intercalation of sPS into the clay gallery. Actually, the direct melt mixing of sPS with 15A induces the contraction of interlayer spacing as shown in Fig. 2. When sPS were melt mixed with 3 wt% of 15A for 5 min, the (001) peak of clay layer appears at $2\theta = 2.93$, which was hardly different from the one of initial state of 15A. The peak around $2\theta = 6.8$–6.9 is the α-form crystal peak of sPS itself. This result means that the obtained product is the conventional microcomposite without any intercalation phenomena between polymer and clay. The increase in mixing time from 5 to 10 min, even induced the contraction of interlayer spacing as the (001) peak appeared around $2\theta = 6.5$ as a small hump. Thus, we attempted to fabricate sPS nanocomposite by the stepwise mixing method mentioned in Section 1.

3.2. Thermal stability of amorphous styrenic polymers/clay nanocomposites

The amorphous styrenic polymers/clay nanocomposites were fabricated as a first step of stepwise mixing method, and their thermal stability was investigated. The nanocomposites with different organophilic clay contents were obtained by melt intercalation in a Brabender roller mixer. Since these nanocomposites would be blended with sPS at above the sPS melting temperature afterwards, the thermal stability should be investigated at this temperature. For this purpose, fabricated nanocomposites were mixed once more in a small vial of mini-molder at 280°C. The change of interlayer spacing for these heat-treated nanocomposites was observed by X-ray diffractometer.

The XRD patterns in Figs. 3–5 show the typical patterns of the intercalated nanocomposite. In the case of aPS and SMA series, the (001) peaks of layered structure shift from $2\theta = 2.97°$ of the original organophilic clay to $2\theta = 2.6$–$2.7°$. The interlayer spacings of clay computed by Bragg's law increase from 2.97 to about 3.4 nm, which is similar to the results by others [9,14,17]. The XRD patterns of SMA

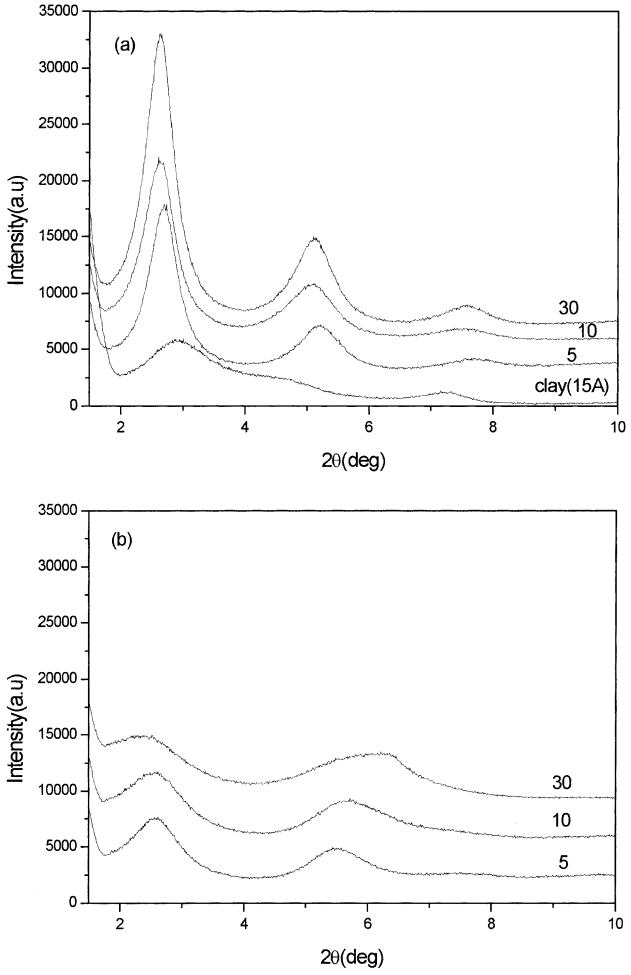

Fig. 3. Variation of XRD patterns of aPS nanocomposite by heat treatment: (a) before heat treatment and (b) after heat treatment (numbers represent the weight percent of clay).

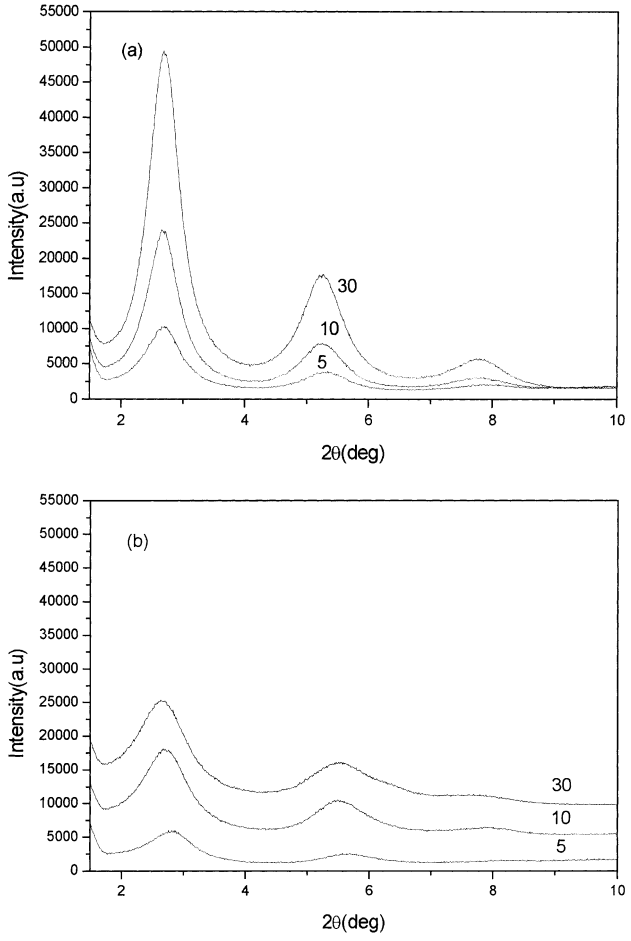

Fig. 4. Variation of XRD patterns of SMA nanocomposite by heat treatment: (a) before heat treatment, and (b) after heat treatment (numbers represent the weight percent of clay).

nanocomposites show similar results with those of aPS nanocomposites. After the heat treatment at 280°C, the intercalation peaks for aPS nanocomposites are decreased and broadened, and a new peak considered as a contracted clay peak appeared around $2\theta = 6.4°$ in the case of nanocomposite with 30 wt% clay. However, in the case of SMA, the intercalation peaks are more distinct than those of aPS nanocomposites after heat treatment. This different behavior of layered structure between aPS and SMA series can be revealed obviously in the XRD patterns with increasing heat treatment times in Fig. 6. The intercalation peak of aPS nanocomposite almost disappeared with increasing heat treatment time whereas SMA nanocomposite retained its intercalation peak. However, the longer heat treatment time of 20 min induces the peak of contracted clay around $2\theta = 6.34°$. It is known that aPS is intercalated in clay layer via weak Lewis acid/base interaction between phenyl group in aPS and clay surface [18]. Heat treatment weakens this interaction so that some portion of aPS exudes from the clay gallery, which leads to the decrease in interlayer spacing. On the other hand, maleic anhydride in SMA making a strong interaction with the hydroxide group in clay surface render the layered structure more firmly in spite of heat treatment.

In the case of SEBS-MA series, the XRD patterns show no peak or broad peak, meaning exfoliated or partially exfoliated structure. The polar character of maleic anhydride interacting with the layer surface aid the penetration of polymer into the clay gallery, whereas the ethylene–butylene blocks are incompatible with the layer surface and repel the clay layer during the intercalation process. This is similar to Hasegawa's result which obtained the exfoliated polypropylene (PP) nanocomposite using maleic anhydride grafted PP (PP-MA) [10]. The theoretical study by Lyatskaya and Balazs also revealed that the incompatibility between polymer and clay (positive Flory–Huggins interaction, $\chi \geq 0$) was required to obtain the exfoliated structure [19]. After heat treatment, the exfoliated structure was retained in nanocomposites with 5 and 10 wt% of clay. This means that already delaminated clay layers exist in individual layers in spite of heat treatment. In the

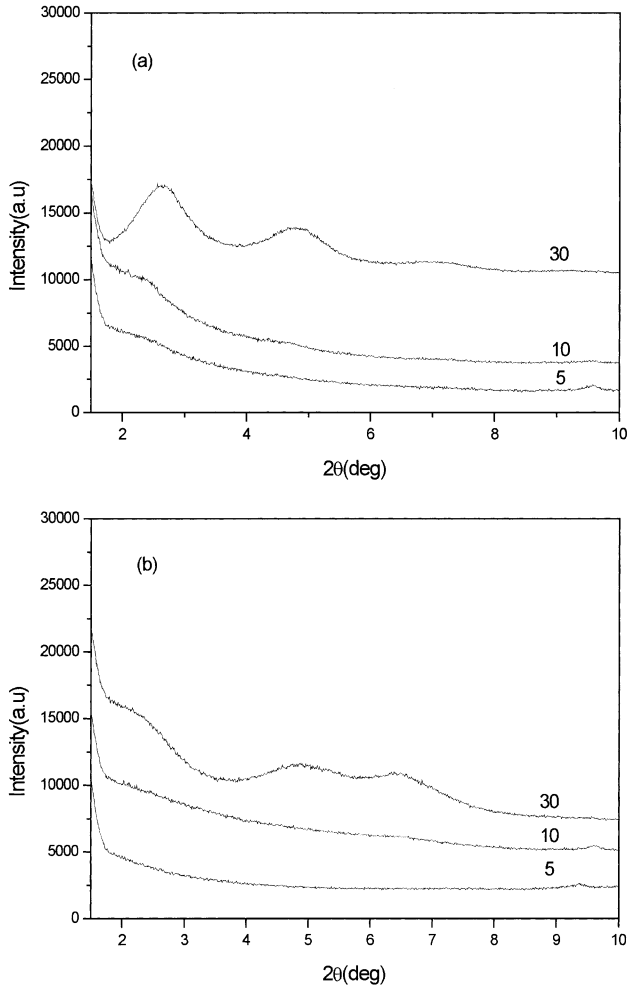

Fig. 5. Variation of XRD patterns of SEBS-MA nanocomposite by heat treatment: (a) before heat treatment and (b) after heat treatment (number represents the weight percent of clay).

case of nanocomposite with 30 wt% clay, the intercalation peak shifted from $2\theta = 2.56$ to 2θ values lower than 1.82, which means almost exfoliated structure. However, the peak of contracted clay also appeared as aPS nanocomposite.

From the above results, it is found that already melt intercalated nanocomposites can keep its intercalated or exfoliated layered structure at sPS melting temperature within 10 min of processing time.

3.3. Microstructure of syndiotactic polystyrene nanocomposite

In the stepwise mixing process, three amorphous styrenic polymer nanocomposites with different organophilic clay contents of 10, 20 and 30 wt% were used. The blend ratio of sPS and amorphous styrenic polymer nanocomposite was 7:3 in all cases. Thus, the organophilic clay contents in sPS nanocomposite were 3, 6 and 9 wt%. In the simultaneous mixing process, the organophilic clay content was 3 wt%. The composition of the sPS nanocomposites is summarized

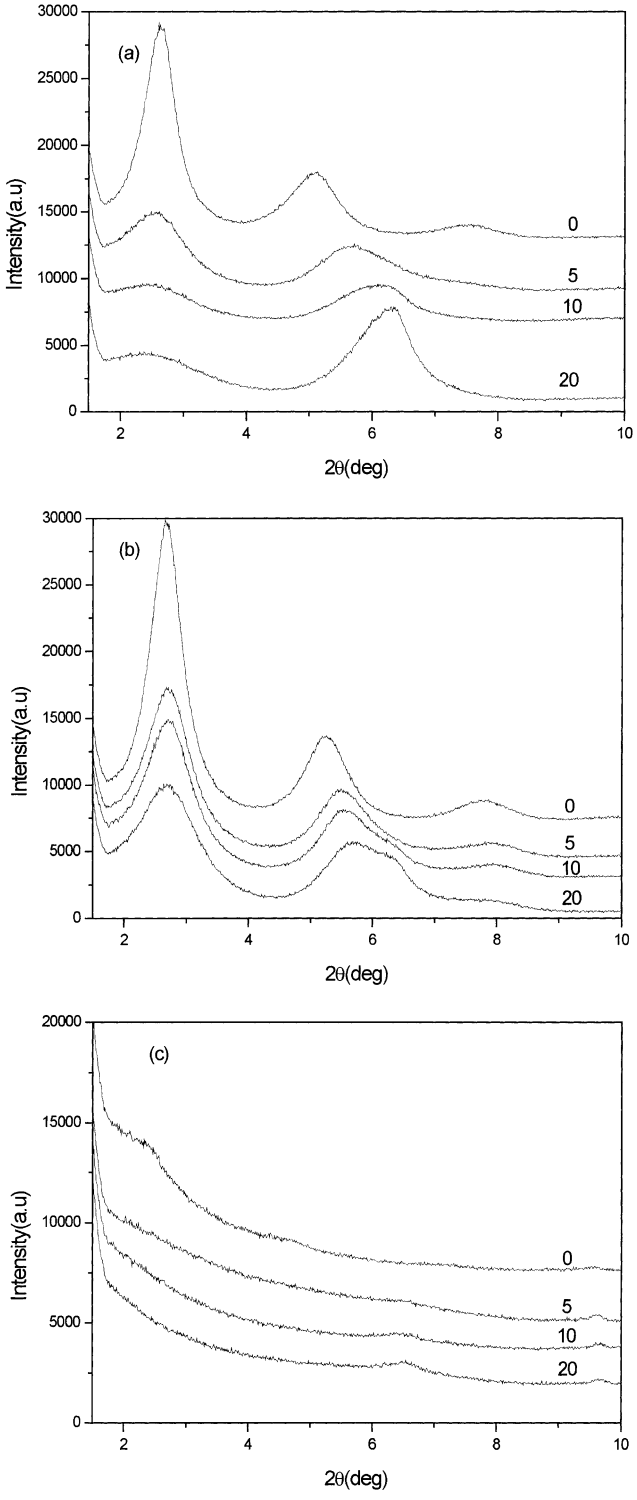

Fig. 6. XRD patterns of styrenic polymer nanocomposites with increasing heat treatment time: (a) aPS nanocomposite, (b) SMA nanocomposite and (c) SEBS-MA nanocomposite (number represents the heat treatment time (min)).

in Table 1. The XRD patterns of fabricated sPS nanocomposite in Figs. 7–9 show intercalation or exfoliation structures as expected in previous thermal stability experiment. The peaks around $2\theta = 6.7$–6.9 known to be the α-form

Table 1
The compositions of sPS nanocomposites and their *d*-spaces

Abbreviation	sPS (wt%)	Amorphous styrenic polymer (wt%)	Organophilic clay, 15A (wt%)	Fabrication method	*d*-space (nm)
SPS	100	0	0	–	–
SPAPS0	70	aPS 30	0	–	–
SPAPS3	70	aPS 27	3	Stepwise	3.52
SPAPS6	70	aPS 24	6	Stepwise	3.44
SPAPS9	70	aPS 21	9	Stepwise	3.60
SPAPS3-1	70	aPS 27	3	Simultaneous	3.56
SPSMA0	70	SMA 30	0	–	–
SPSMA3	70	SMA 27	3	Stepwise	3.25
SPSMA6	70	SMA 24	6	Stepwise	3.33
SPSMA9	70	SMA 21	9	Stepwise	3.29
SPSMA3-1	70	SMA 27	3	Simultaneous	3.33
SPKMA0	70	SEBS-MA 30	0	–	–
SPKMA3	70	SEBS-MA 27	3	Stepwise	exfoliation
SPKMA6	70	SEBS-MA 24	6	Stepwise	3.37
SPKMA9	70	SEBS-MA 21	9	Stepwise	3.38
SPKMA3-1	70	SEBS-MA 27	3	Simultaneous	exfoliation

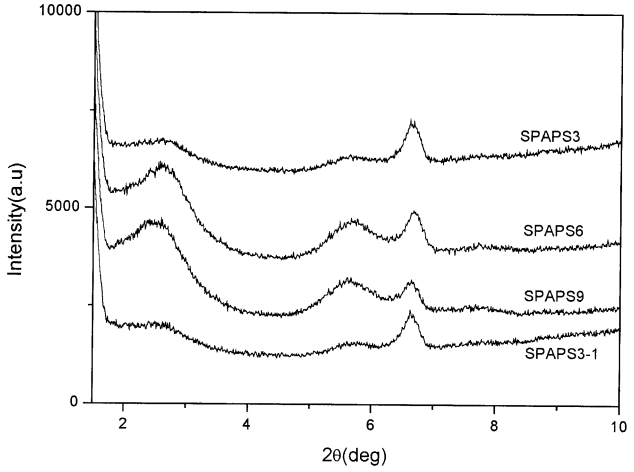

Fig. 7. XRD patterns of sPS nanocomposite using aPS as an amorphous polymer (refer to Table 1 for abbreviations).

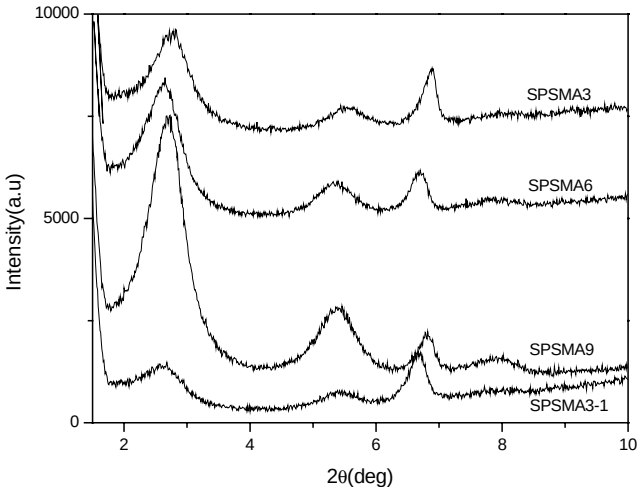

Fig. 8. XRD patterns of sPS nanocomposite using SMA as an amorphous polymer (refer to Table 1 for abbreviations).

crystal peak of sPS are also seen in the figure. In the case of using aPS or SMA as an amorphous polymer, the intercalation peak with increased (001) *d*-space is observed. The intercalation peaks of SMA series are more distinct than those of aPS series due to the interaction between maleic anhydride and clay layer surface. In the SEBS-MA series, the exfoliation structure was obtained in nanocomposite with 3 wt% organophilic clay. By increasing the clay content, the broad intercalation peak appears, which means the exfoliation occurs partially due to the high amount of clay. By the way, we could obtain one notable result that the XRD patterns of the nanocomposites by simultaneous mixing are almost the same as those of nanocomposites by stepwise mixing. It is known that the kinetics of melt intercalation depends on the diffusion coefficient of polymer. In case of aPS, the diffusion coefficient at 280°C is

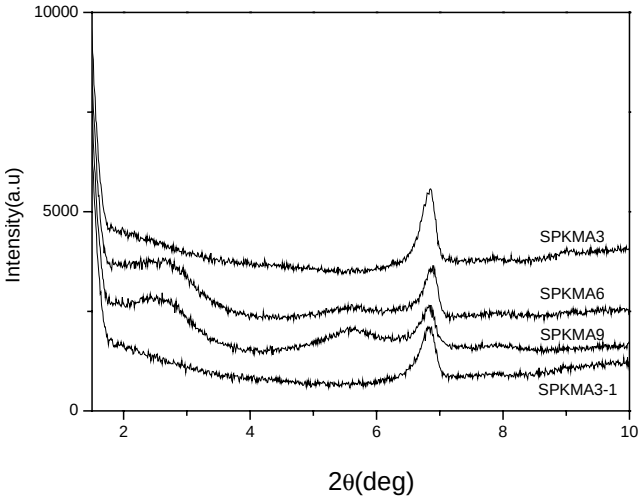

Fig. 9. XRD patterns of sPS nanocomposite using SEBS-MA as an amorphous polymer (refer to Table 1 for abbreviations).

about 500 times higher than that at 200°C of common processing temperature, assuming the Arrhenius temperature dependence of diffusion coefficient with the activation energy of 167 kJ/mol reported by Vaia et al. [20]. Therefore, in the simultaneous mixing method, the diffusion coefficient of amorphous polymer used here increases greatly so that the amorphous polymer may diffuse into the clay gallery very rapidly before the contraction of the interlayer spacing. This result indicates that the use of amorphous styrenic polymer is inevitable for the fabrication of sPS nanocomposite, irrespective of the type of fabrication method.

The microstructures of sPS nanocomposites observed by TEM are shown in Fig. 10. The layered structure of clay intercalated by polymer is shown in aPS and SMA series. However, a slight difference in the clay structure between the two fabrication methods could be observed. The layered structure of clay intercalated by polymer in the stepwise mixing method is obvious in comparison to the layered structure in simultaneous mixing method. It seems that the dispersion of clay is rather poor locally in simultaneous mixing method since it is mixed once, whereas it is mixed twice in stepwise mixing method. Another reason seems to be the degradation of alkylammonium chain in some portion of clay followed by the decrease in interlayer spacing at high temperature even though this agglomerate portion is not detected in XRD patterns. In the case of SEBS-MA series, the individual clay layers are dispersed completely, which is a typical exfoliated structure. No difference could be observed between the two fabrication methods.

3.4. Mechanical properties of syndiotactic polystyrene nanocomposite

Tensile strength, flexural modulus and izod impact strength were measured as mechanical properties. At first, the mechanical properties of the blend of sPS with amorphous styrenic polymers were measured as reference data. When sPS is blended with aPS or SMA, the tensile strength shows a lot of decrease in Fig. 11. In general, the crystal structure such as a spherulite in sPS plays an important role in its mechanical properties. This spherulite structure is known to disrupt by blending with miscible amorphous polymer like aPS or SMA, which affects the tensile strength negatively [21]. As the content of clay increases, the tensile

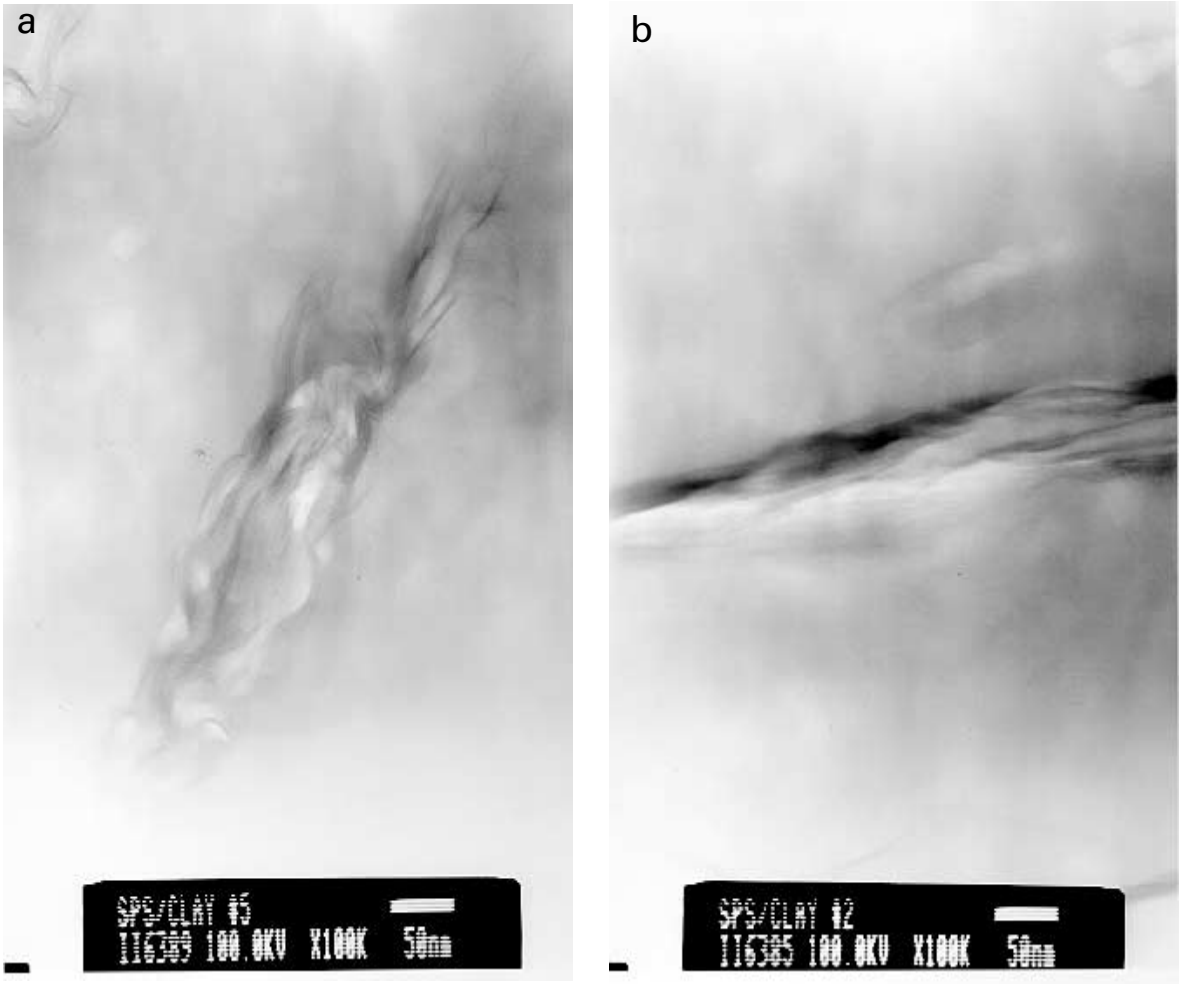

Fig. 10. TEM of sPS nanocomposites: (a) SPAPS3, (b) SPAPS3-1, (c) SPSMA3, (d) SPSMA3-1, (e) SPKMA3 and (f) SPKMA3-1.

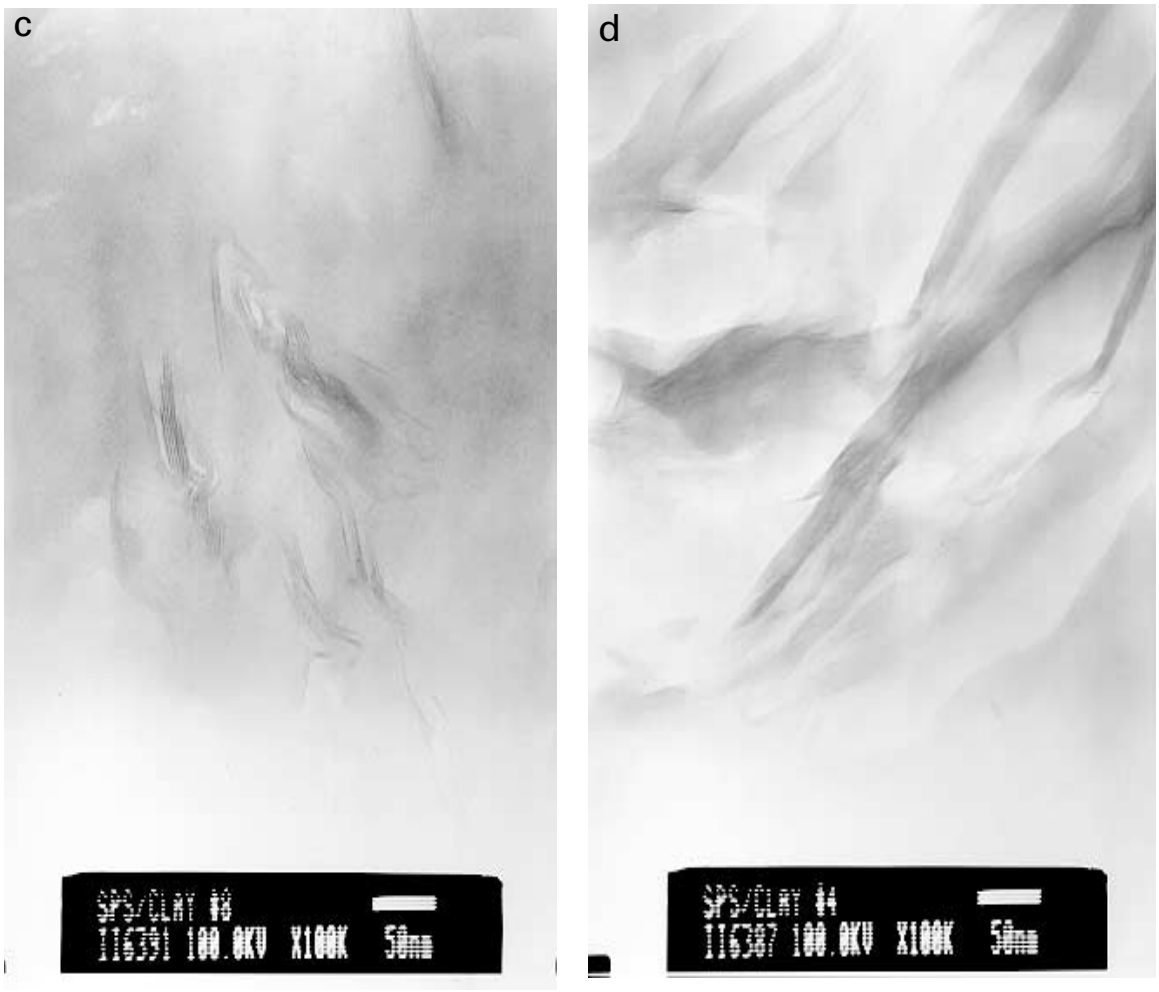

Fig. 10. (*continued*)

strength of nanocomposite increases greatly due to nano-scaled hybrid of polymer and clay. However, the nanocomposites fabricated by the simultaneous mixing method show lower tensile strengths than the nanocomposites made by the stepwise mixing method. Some portion of clay, which are not involved in polymer/clay hybrid in the simultaneous mixing method may cause defects in tensile strength as explained in TEM observation. The tensile strength of the nanocomposite using SEBS-MA increases slightly with the increase in clay contents. In this case, a large portion of clay layer remains in SEBS-MA phase because SEBS-MA forms a domain in sPS matrix so that the reinforcing effect of clay is rather low in comparison to the aPS and SMA series. There is little difference between the two fabrication methods since almost all clay layers exist in exfoliated state in both methods as observed by TEM. Flexural modulus also increases with the increase in clay contents in all cases in Fig. 12. The SEBS-MA series shows lower flexural modulus than sPS itself due to the elastic characteristic of SEBS-MA and both fabrication methods show similar results. Flexural modulus is not largely affected by the small defect like tensile strength since modulus is not the property at break, but initial property in stress–strain curve. Improved impact strength is obtained in SEBS-MA series due to the elastic characteristic of SEBS-MA (Fig. 13). However, the nanocomposite with 3 wt% of clay (SPKMA3 and SPKMA3-1) even shows impact strength higher than the blend of sPS and SEBS-MA in spite of the existence of inorganic filler. This means that the exfoliated clay layers in nanocomposite play a role in disturbing the crack path caused by impact.

4. Conclusions

The fabrication of sPS nanocomposite was conducted by the melt intercalation method. In order to avoid the thermal instability problem of organophilic clay, various amorphous styrenic polymers were introduced. By using amorphous styrenic polymers during the melt mixing process, sPS nanocomposite could be obtained successfully in both fabrication methods: stepwise mixing method and simultaneous mixing method. Amorphous polymers intercalated into the clay gallery previously is considered to play an important

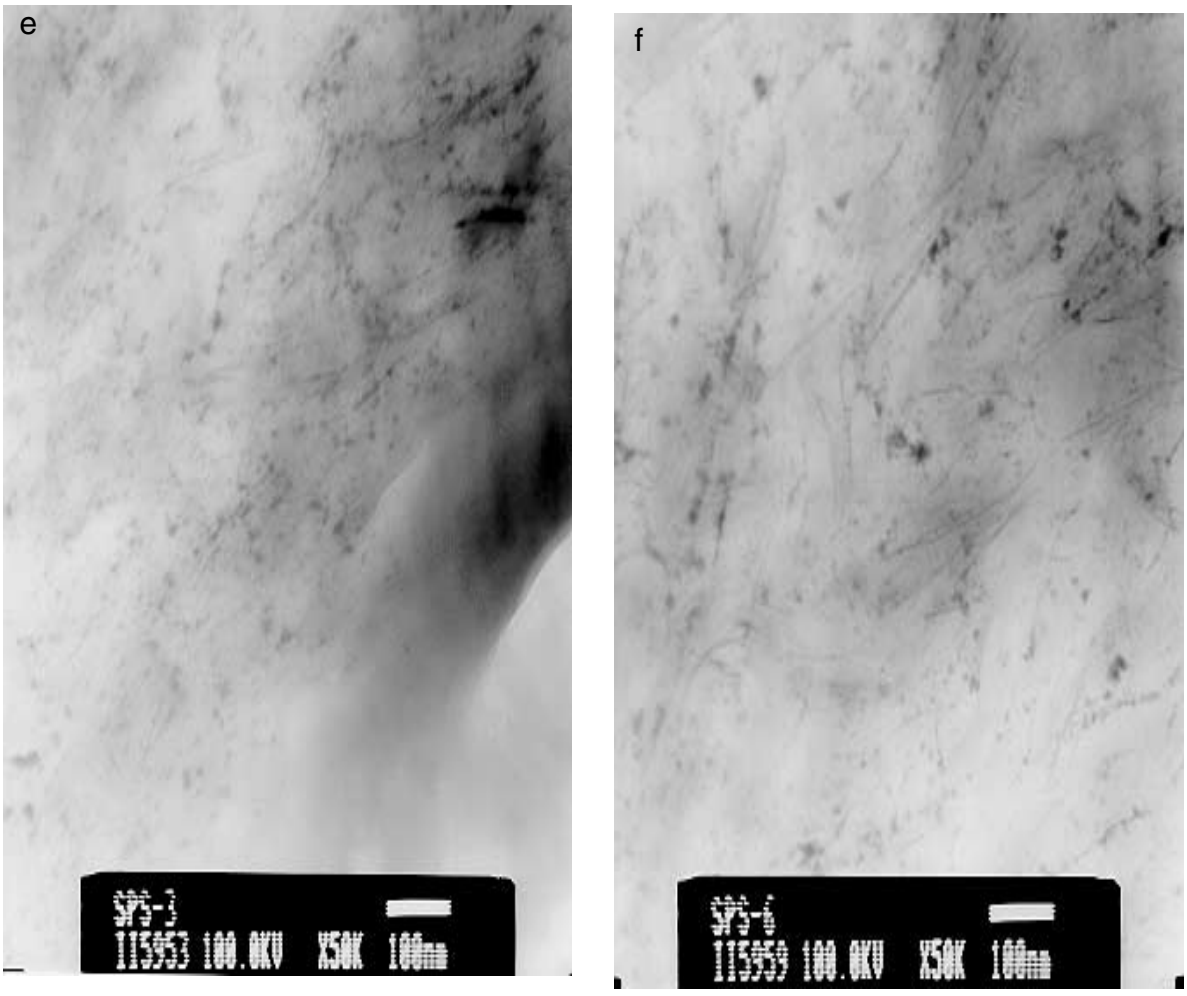

Fig. 10. (*continued*)

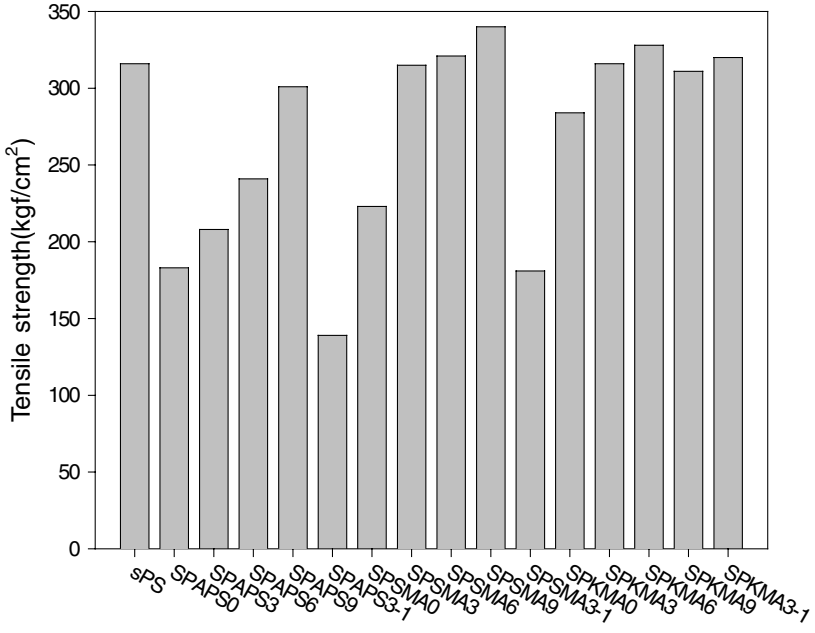

Fig. 11. Tensile strength of sPS nanocomposites (refer to Table 1 for abbreviations).

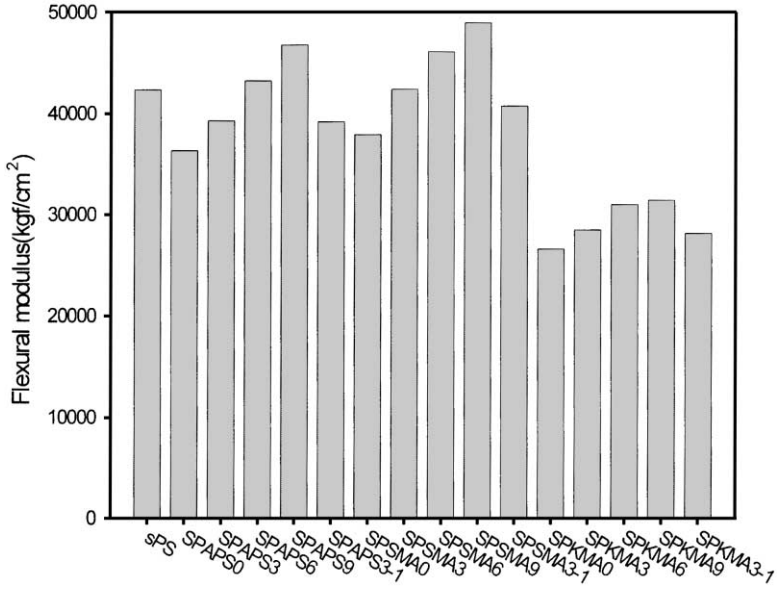

Fig. 12. Flexural modulus of sPS nanocomposites (refer to Table 1 for abbreviations).

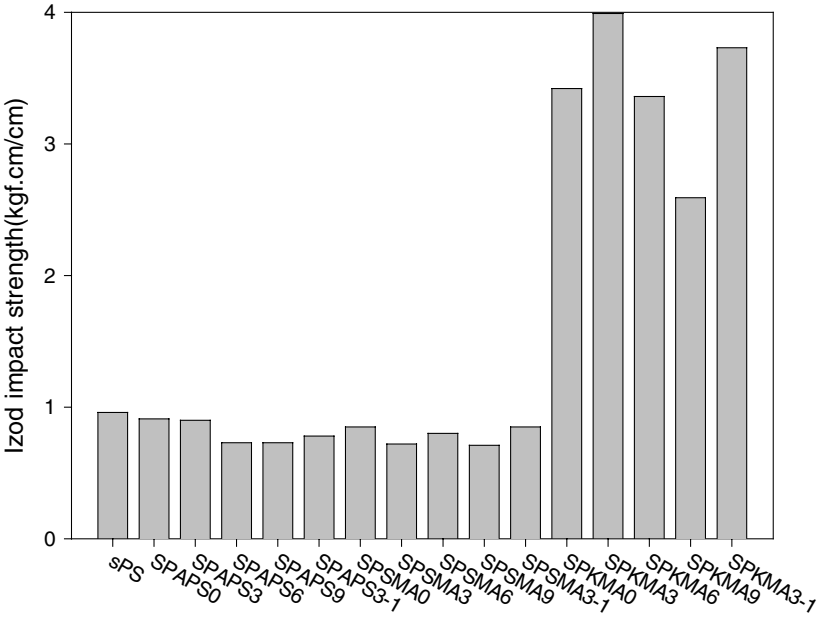

Fig. 13. Izod impact strength of sPS nanocomposites (refer to Table 1 for abbreviations).

role in maintaining the intercalated or exfoliated structure without any contraction of interlayer spacing even at sPS melting temperature. One notable result is that the pre-melt intercalation of amorphous polymers is possible even in the simultaneous mixing method as well as the stepwise mixing method because of the great increase in diffusion coefficient at high processing temperatures. The microstructures of the nanocomposites depend on the kind of amorphous styrenic polymers. Nanocomposites using SMA have firmer intercalation structure than those using aPS due to the interaction of maleic anhydride with layer surface of clay, and the exfoliated structure is obtained in nanocomposites using SEBS-MA. The improvement of mechanical properties is observed by accomplishing the nanoscaled hybrid between polymer and clay. However, there is a difference between the two fabrication methods in view of the tensile strength. The stepwise mixing method is more favorable than the simultaneous mixing method in the case of the occurrence of intercalation structure since the former method yields more complete intercalation structure. On the other hand, the nanocomposites having exfoliated structure show similar mechanical properties in both fabrication methods. Thus,

the simple simultaneous mixing method is more favorable in this exfoliated case. However, to improve the mechanical properties further, more study on the optimization of composition is still needed.

Acknowledgements

The authors are very grateful for the financial support provided by Samsung General Chemical Ltd. This work is also partially supported by the Brain Korea 21 project of the Ministry of Education (MOE) of Korea.

References

[1] LeBaron PC, et al. Appl Clay Sci 1999;15:11–29.
[2] Giannelis EP, et al. Adv Polym Sci 1999;138:107–47.
[3] Kojima Y, et al. J Sci Polym Chem Ed 1993;31:983–6.
[4] Kojima Y, et al. J Polym Sci Polym Chem Ed 1993;31:1755–8.
[5] Lan T, et al. Chem Mater 1995;7:2144–50.
[6] Yano K, et al. J Polym Sci Polym Chem Ed 1993;31:2493–8.
[7] Suh DJ, et al. Polymer 2000;41:8557–63.
[8] Messersmith PB, Giannelis EP. J Polym Sci Polym Chem Ed 1995;33:1047–57.
[9] Sikka M, et al. J Polym Sci Polym Phys Ed 1996;34:1443–9.
[10] Hasegawa N, et al. J Appl Polym Sci 1998;67:87–92.
[11] Ishihara N, et al. Macromolecules 1986;19:2464–5.
[12] Lee JW, et al. Polym Bull 2000;45:191–8.
[13] Gilman JW, et al. Chem Mater 2000;12:1866–73.
[14] Vaia RA, et al. Chem Mater 1993;5:1694–6.
[15] Woo EM, et al. Polymer 2000;41:883–90.
[16] Ermer H, et al. Macromol Chem Phys 1997;198:3639–45.
[17] Lim YT, Park OO. Macromol Rapid Commun 2000;21:231–5.
[18] Vaia RA, et al. Macromolecules 30 1997:8000–9.
[19] Lyatskaya Y, Balazs AC. Macromolecules 1998;31:6676–80.
[20] Vaia RA, et al. Macromolecules 1995;28:8080–5.
[21] Bonnet M, et al. Polym Bull 1999;42:353–6.